



Performance of $\text{La}_{0.9}\text{Sr}_{0.1}\text{Ga}_{0.5}\text{Ni}_{0.5}\text{O}_3$ as a Cathode for a Lanthanum Gallate Fuel Cell

FRÉDÉRIC LECARPENTIER,¹ HARRY L. TULLER² & NICK LONG¹

¹Industrial Research Limited, Gracefield Road, PO Box 31-310, Lower Hutt, New Zealand

²Crystal Physics and Electroceramics Laboratory, Department of Materials Science and Engineering, Massachusetts Institute of Technology, Cambridge, MA 02139, USA

Submitted April 1, 1999; Revised May 10, 2000; Accepted May 11, 2000

Abstract. The cathodic overpotential of a $\text{La}_{0.9}\text{Sr}_{0.1}\text{Ga}_{0.5}\text{Ni}_{0.5}\text{O}_3$ (LSGN) electrode on a $\text{La}_{0.9}\text{Sr}_{0.1}\text{Ga}_{0.8}\text{Mg}_{0.2}\text{O}_3$ (LSGM) electrolyte was studied using the current interruption technique. The electrode performance was found to be clearly superior to $\text{La}_{0.85}\text{Sr}_{0.15}\text{MnO}_3$ and comparable to $\text{La}_{0.6}\text{Sr}_{0.4}\text{CoO}_3$ in the temperature range of 700–850°C. The exchange current density is a maximum in air and is smaller in either 100% O_2 or 2% O_2 suggesting that the occupation of surface adsorption sites is important. The overpotential-current density curves suggest that charge transfer is the limiting process for high current densities. An energy dispersive spectrometry line scan did not show any significant interdiffusion of Ni ions across the electrode/electrolyte boundary.

Keywords: lanthanum gallate, fuel cell cathode, mixed conductor

1. Introduction

Solid oxide fuel cells (SOFC) operating at temperatures below 800°C would minimize materials degradation and enable the use of lower cost components [1]. The discovery of the lanthanum gallate electrolyte, $\text{La}_{1-y}\text{Sr}_y\text{Ga}_{1-x}\text{Mg}_x\text{O}_{3-\delta}$ (LSGM), with high ionic conductivity at intermediate temperatures [2,3], gives considerable impetus to this area of research. $\text{La}_{0.9}\text{Sr}_{0.1}\text{Ga}_{0.8}\text{Mg}_{0.2}\text{O}_{3-\delta}$ has an ionic conductivity of 0.1 S/cm at 800°C [2,3]. Following the assumptions by [4] that the cell resistance should be less than $0.3 \Omega \text{cm}^2$ we can calculate that an LSGM electrolyte with a thickness of 150 μm or less would make the electrode performance rate limiting. Therefore, to take full advantage of the LSGM electrolyte, compatible electrode materials, capable of operating at reduced temperatures with low overpotentials, are required.

The most studied cathode materials for the YSZ electrolyte are the perovskites $\text{La}_{1-x}\text{Sr}_x\text{MnO}_3$ (LSM) and $\text{La}_{1-x}\text{Sr}_x\text{CoO}_3$ (LSC). LSM has been shown to have a low catalytic activity for oxygen

reduction when used with the LSGM electrolyte at lower temperatures [5]. LSC has superior exchange current densities, likely due to mixed conductivity, but interdiffusion of elements may cause the formation of non-conductive phases and thermal expansion mismatch may result in mechanical degradation [5,6]. Finding a new cathode material with full compatibility with LSGM is required to exploit this new electrolyte.

Earlier, we reported that Ni-substituted lanthanum gallates are mixed ionic/electronic conductors with sufficient levels of ionic and electronic conductivity required for fuel cell cathode operation [7,8]. Here we report results of overpotential studies performed on a cathode of $\text{La}_{0.9}\text{Sr}_{0.1}\text{Ga}_{0.5}\text{Ni}_{0.5}\text{O}_3$ (LSGN) applied on to LSGM. LSGN has a hexagonal crystal structure with $a = 5.497 \text{ \AA}$ and $c = 6.634 \text{ \AA}$. The total conductivity at 800°C in air is $\sim 50 \text{ S/cm}$. Thermal expansion measurements show a good fit to the electrolyte in the range 20–800°C [7,8]. We compare these results with our own measurements on LSC and LSM cathodes and those made by previous researchers [5,6].

2. Experimental

$\text{La}_{0.9}\text{Sr}_{0.1}\text{Ga}_{0.5}\text{Ni}_{0.5}\text{O}_3$ was prepared by solid-state synthesis using high purity (99.99%) oxide powders of La_2O_3 , SrCO_3 , Ga_2O_3 , and NiO . The powders were mixed in an agate mortar, then pelletized and fired 3 times at 1300°C for 16 h with intermediate regrinding. A final firing was performed at 1500°C for 4 h. An XRD analysis showed the formation of the LSGN compound without impurity phases. To prepare an electrode paste, the pellets were crushed to give a coarse powder and the powder was then micronized using a jet-mill. The particle size distribution of the LSGN powder, obtained from a Shimadzu SALD-2001 laser light scattering instrument, is shown in Fig. 1. The median particle size was $1.7\ \mu\text{m}$; this powder (3.5 g) was then mixed with an organic vehicle (2.5 g - Decal Medium; Johnson Matthey, Colour and Print Division, Victoria 3172, Australia, ref 7340/S) and turpentine (1 ml) to form an ink.

The LSC and LSM powders formed by the glycine-nitrate combustion synthesis method [9] had an average particle size of about $0.6\ \mu\text{m}$. The results from laser light scattering were not accurate due to agglomeration but the method is known to produce a narrow size distribution. The compositions were

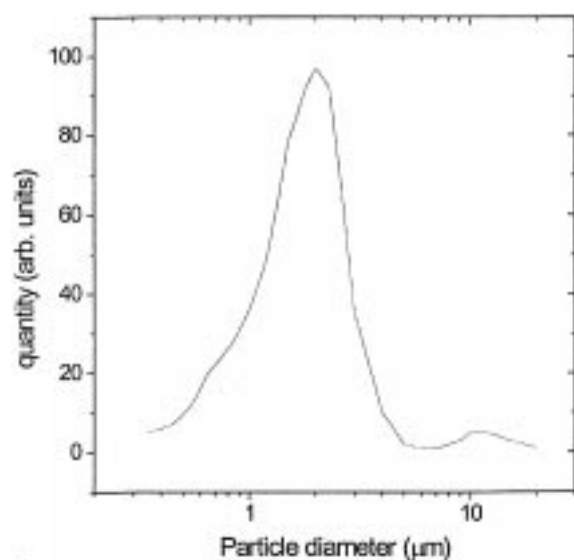


Fig. 1. Particle size distribution of jet-milled LSGN powder.

$\text{La}_{0.6}\text{Sr}_{0.4}\text{CoO}_3$ and $\text{La}_{0.85}\text{Sr}_{0.15}\text{MnO}_3$. They were mixed with organic vehicle and solvent to form an ink in the same way as the LSGN powder.

The LSGM electrolyte was synthesized using the same procedure as the LSGN, with MgO rather than NiO . The jet-milled powder was uniaxially pressed into a disk of 15 mm diameter and 0.8 mm thickness, and then isopressed at 350 MPa before being sintered at 1500°C for 36 h. The pellets were 99% of the theoretical density of $6.66\ \text{g/cm}^2$. The electrode ink was then applied to both sides of the sample to form the working and counter electrodes and reference electrode. Reference electrodes were formed on both sides of the pellet so that a symmetric configuration was maintained. The electrode arrangement is shown schematically in Fig. 2. The symmetric configuration has been shown to lead to more reliable overpotential measurements [10]. LSC and LSM electrodes were sintered at 1100°C for 4 h. The LSGN electrodes were sintered at 1400°C for 2 h. This sintering temperature gave good adhesion between the LSGN and electrolyte. Electrodes sintered at lower temperature, such as 1100°C , did not adhere well and could be easily scraped off with a sharp object such as tweezers. Once sintered, platinum mesh current collectors were affixed to the counter and working electrodes with Pt paste to provide good electrical contact.

The cathodic polarization was measured by the current interruption technique using a current supply (Yokogawa 7651), a fast reed relay, and a digital oscilloscope (Tektronix TDS430A). Measurements were made in air, 100% O_2 and 2% O_2 in N_2 at temperatures from 700 to 850°C .

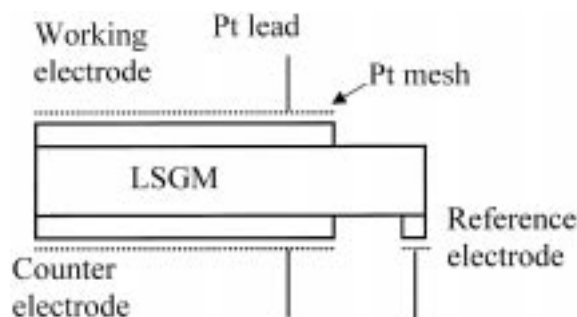


Fig. 2. Symmetric electrode arrangement of experimental cell.

3. Results and Discussion

Figure 3 shows a typical SEM micrograph of the electrode/electrolyte interface. The electrode has good porosity and is approximately 85 μm thick. An energy dispersive spectrometry (EDS) line scan measured across the LSGN/LSGM interface, shown in Fig. 4, shows the spatial intensity of the Ni and Mg signals. The grain size in the electrode is about 15 μm . The scan shows three regions, (i) where there is no signal, (ii) the LSGN grain region and then (iii) the LSGM bulk region. The width of the transition region from electrode to electrolyte is about 5 μm showing that the Ni has not diffused significantly from the electrode into the electrolyte. This is not the case with LSC electrodes where significant interdiffusion of Co has been observed [6].

Figure 5 is a current interruption trace used to separate the overpotential and IR contributions to the total voltage between the reference and working electrodes. A comparison of the overpotential versus current density for LSM, LSC and LSGN in air at 800°C is shown in Fig. 6. We assume that the electrode process is linear at small overpotentials and therefore define the exchange current density i^o using the formula

$$\eta = \frac{RT}{nFi^o} i \tag{1}$$

where η is the overpotential, i the current density, and $n = 2$ is the charge transferred per oxide ion. The results for i^o calculated from the low overpotential

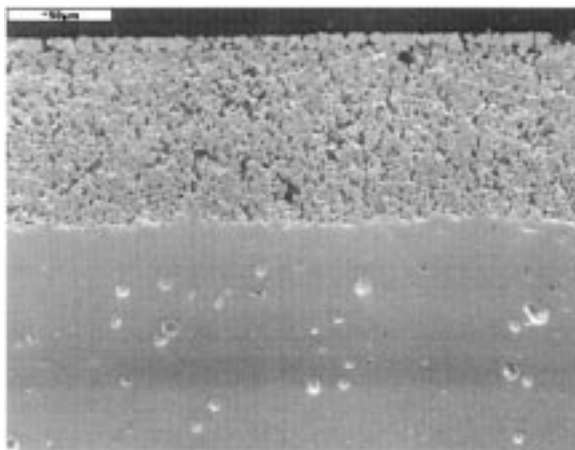


Fig. 3. SEM micrograph of porous LSGN electrode on LSGM electrolyte.

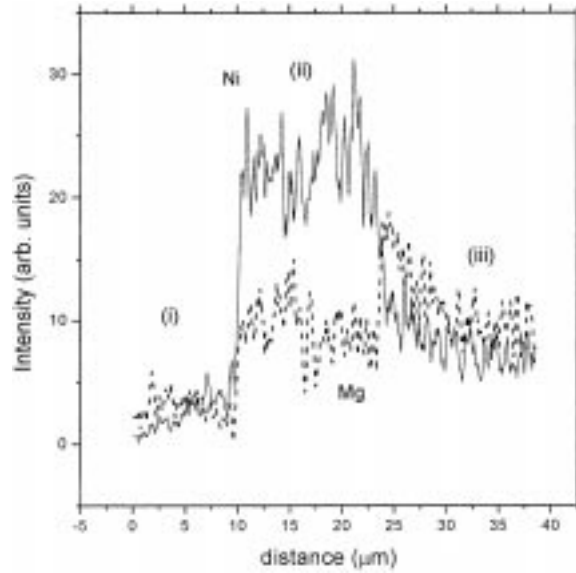


Fig. 4. EDS linescan showing the Ni and Mg signals as a function of position.

linear part of the curves in Fig. 6 are summarized in Table 1. The results for LSM are comparable with those of Huang et al. [5]. Our current density for LSC is lower by a factor of about five. This may be due to differences in our electrode preparation giving a different morphology. The results for LSGN are

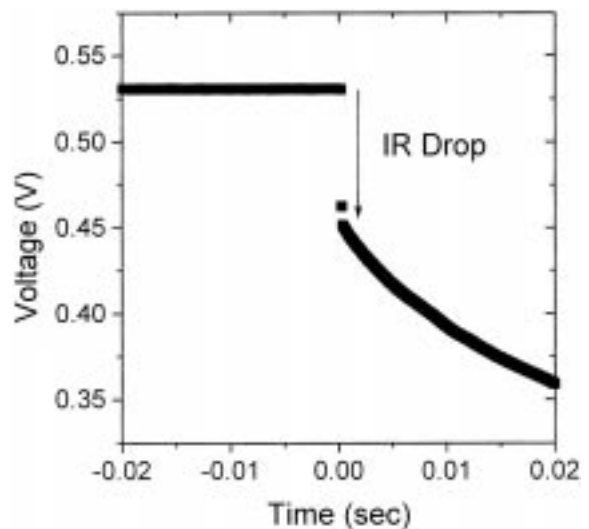


Fig. 5. Current interruption curve showing the IR drop.

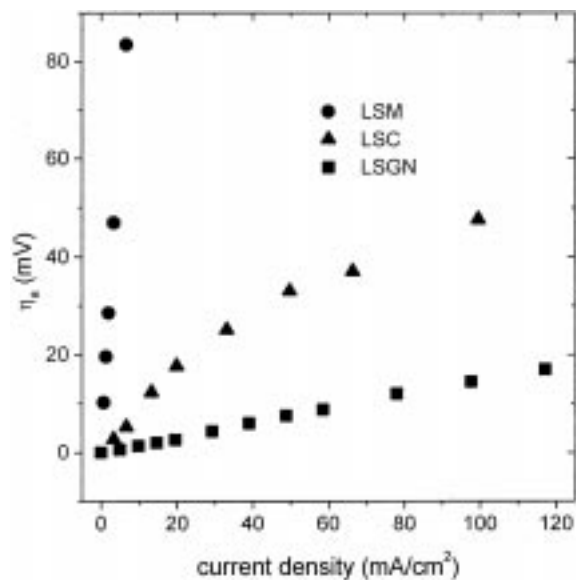


Fig. 6. A comparison of cathode overpotentials in air at 800°C, for samples of LSM, LSC and LSGN on a LSGM electrolyte.

superior at 800°C to LSC, suggesting that this material has an excellent catalytic performance as a cathode for an LSGM fuel cell. The results for the overpotential measurements in air are shown in Fig. 7. These are fitted to the usual Butler-Volmer equation

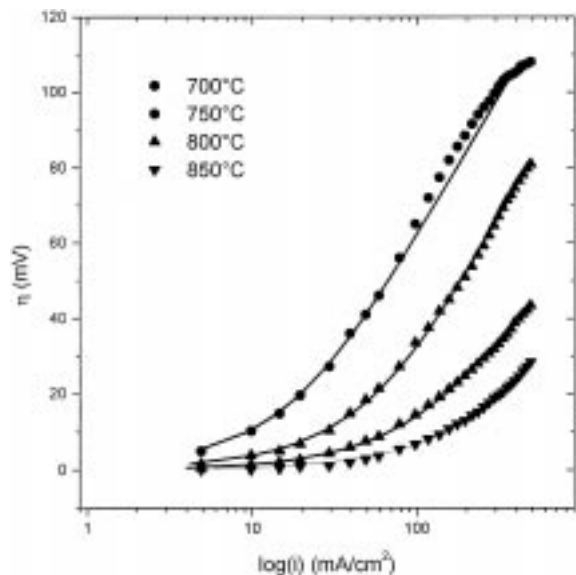


Fig. 7. Tafel plots for the cathodic overpotential of LSGN in air. The solid curves are fits to the Butler-Volmer equation.

$$i = i_0[\exp(\alpha_a \eta F/RT) - \exp(-\alpha_c \eta F/RT)]$$

where we have set the exchange coefficients $\alpha_a = \alpha_c$. The good fit obtained suggests that the charge transfer process is rate limiting. At high overpotentials and low temperatures there is some deviation from the Butler-Volmer form, in this region solid state or gas phase mass transfer may become important.

In order to investigate the oxygen reduction further, we measured the variation of the exchange current density with P_{O_2} as shown in Fig. 8. This shows that the exchange current is a maximum in air and is smaller at lower and higher P_{O_2} . This behavior may reflect a Langmuir type adsorption where

$$i_0 \sim [\theta(1 - \theta)]^{1/2} \quad (2)$$

where θ is the concentration of occupied surface adsorption sites. For Langmuir adsorption, a $P_{O_2}^{1/4}$ or $P_{O_2}^{-1/4}$ dependence is possible depending on whether θ is small or large respectively. The maximum in the exchange current could reflect that $\theta \sim 1/2$ for $P_{O_2} \sim 0.21$ atm. for the LSGN cathode. According to a recent model of the performance of mixed conducting electrodes, the reaction zone is limited to a few microns beyond the three phase boundary [11]. If this model is valid then most of our electrode does not contribute to oxygen reduction. The large thickness of the electrode may result in a gas phase limited diffusion, which would give a $P_{O_2}^{+1}$ dependence in the exchange current

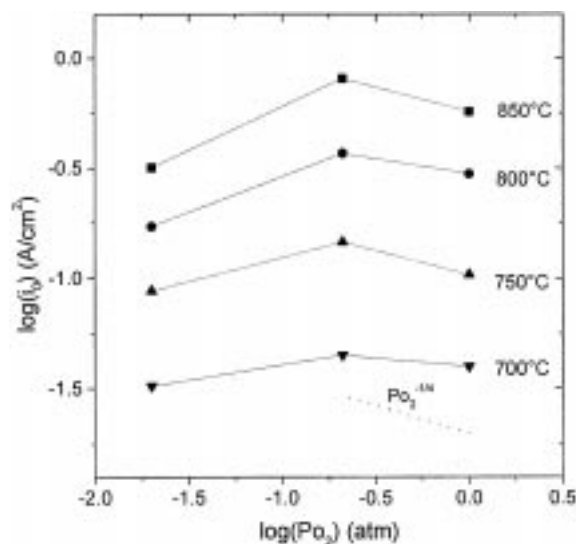


Fig. 8. The P_{O_2} dependence of the exchange current density for the LSGN cathode. The slope for $P_{O_2}^{-1/4}$ is indicated on the graph.

Table 1. Properties of electrodes on LSGM electrolyte

Electrode	i_0 (A/cm ²) (800°C)	E_A (eV)	Ref.
La _{0.6} Sr _{0.4} CoO ₃	0.263	0.96	Huang
La _{0.6} Sr _{0.4} CoO ₃	0.05	—	This work
La _{0.85} Sr _{0.15} MnO ₃	0.003	—	Huang
La _{0.85} Sr _{0.15} MnO ₃	0.004	—	This work
La _{0.9} Sr _{0.1} Ga _{0.5} Ni _{0.5} O ₃	0.368	1.816	This work

[11]. As this is not the case, we conclude that gas phase diffusion is not a limiting factor.

The activation energy for the exchange current density was found to be 1.82 eV in air. This is much higher than the activation energy of the LSC electrode on LSGM of approximately 1 eV calculated from the results of Huang et al. [5], but is lower than that found by Takeda et al. [12] for LSC on YSZ of 2.2 eV. Activation energies and the P_{O_2} dependencies of perovskite cathodes vary with the B site cation. This probably reflects two main characteristics, the catalytic ability for the oxygen gas dissociation and the degree of oxygen ion conductivity. A degree of oxygen ion conductivity allows the expansion of the reactive surface area to the whole surface of the cathode rather than only the triple phase boundary. The good performance of LSC has been widely attributed to its mixed conductivity. We speculate that the similar performance of the LSGN cathode is due to the mixed conductivity in this material. Accurately measuring the ionic conductivity in a material with dominant electronic conductivity is difficult. We have shown that the material La_{0.9}Sr_{0.1}Ga_{0.8}Ni_{0.2}O₃ has a high ionic conductivity using AC impedance spectroscopy [7]. However due to overlapping features in the impedance spectrum we were not able to get an accurate value for the ionic conductivity of La_{0.9}Sr_{0.1}Ga_{0.5}Ni_{0.5}O₃ using this method.

Conclusions

LSGN shows good performance as a cathode for a LSGM electrolyte fuel cell. The catalytic performance is superior to LSM and comparable to LSC. An analysis of the overpotential results suggests that oxygen adsorption and charge transfer effects are important. The low overpotential despite a high activation energy suggests a large surface area for the reaction due to the mixed conductivity of the electrode. EDS line scan analysis has shown that there

is no significant interdiffusion of the Ni cations into the electrolyte.

Acknowledgments

N.J. Long thanks the New Zealand Foundation for Research Science and Technology for financial support. H.L. Tuller thanks the Basic Energy Sciences Division of the U.S. Department of Energy under contract DE FG02 86ER 45261 for its assistance.

References

1. H.L. Tuller, "Ionic and Mixed Conductors: Materials Design and Optimization," in *High Temperature Electrochemistry: Ceramics and Metals* edited by F.W. Poulsen, N. Bonanos, S. Linderth, M. Mogensen, and B. Zachau-Christiansen (Risø National Laboratory, Roskilde, Denmark, 1996), p. 139.
2. T. Ishihara, H. Matsuda, and Y. Takita, *J. Amer. Chem. Soc.*, **116**, 3801 (1994).
3. M. Feng and J.B. Goodenough, *Eur. J. Solid State Chem.*, **31**, 663 (1994).
4. B.C.H. Steele, *Solid State Ionics*, **75**, 157 (1995).
5. K. Huang, M. Feng, J.B. Goodenough, and C. Milliken, *J. Electrochem. Soc.*, **144**, 3620 (1997).
6. K. Huang, M. Feng, J.B. Goodenough, and M. Schmerling, *J. Electrochem. Soc.*, **143**, 3630 (1996).
7. N.J. Long and H.L. Tuller, "Mixed Ionic-Electronic Conduction in Ni-Doped Lanthanum Gallate Perovskites," in *Materials for Electrochemical Energy Storage and Conversion II - Batteries, Capacitors and Fuel Cells*, (MRS vol. 496) edited by D. Ginley, D. Doughty, B. Scrosati, T. Takamura, and Z. Zhang (Materials Research Society, Warrendale, PA, 1998), pp. 129–137.
8. N.J. Long, F. Lecarpentier, and H.L. Tuller, *J. Electroceramics*, **3:4**, 399–407 (1999).
9. L.A. Chick, L.R. Pederson, G.D. Maupin, J.L. Bates, L.E. Thomas, and G.J. Exarhos, *Materials Lett.*, **10**, 6 (1990).
10. M. Nagata, Y. Itoh, and H. Iwahara, *Solid State Ionics*, **67**, 215 (1994).
11. S.B. Adler, J.A. Lane, and B.C.H. Steele, *J. Electrochem. Soc.*, **143**, 3554 (1996).
12. Y. Takeda, R. Kanno, M. Noda, Y. Tomida, and O. Yamamoto, *J. Electrochem Soc.*, **134**, 2656 (1987).